

Geometry factor for near surface borehole resistivity surveys: a key to accurate imaging and monitoring

Kun Guo¹, Bernd Milkreit¹ and Wei Qian²

¹Department of Earth Sciences, University of Toronto

²Geoserve Logging & Tomography

Summary

Under ideal conditions, resistivity measurements should be fully repeatable and able to monitor time varying changes. However, data acquisition system mislocations as well as borehole deviation effects can raise signification errors that are problematic in imaging and monitoring target structures. Such errors can be potentially accounted for by obtaining correct geometry factors. A resistivity profiling survey was conducted under a lake and the importance of geometry factors in apparent resistivity is investigated by comparing results with and without taking deviation effect into account.

Introduction

For near surface Earth materials within lithostatic pressure, bulk resistivity is not only controlled by conductive materials, but largely influenced by porosity, permittivity, fracturing and fluid content (Ward, 1990). In general, porosity, permittivity and fracturing would increase the rock's resistivity. Fluid induced into these open spaces, however, may further complicate the situation by either increasing (oil) or decreasing (water) the bulk resistivity. Therefore, changes in bulk resistivity can be used as a good indicator of changes in stress and structures. Over the last century, surface resistivity surveys have been well utilized. Nevertheless, electrodes planted on the surface can be heavily influenced by weather, temperature, and water saturation changes over time. Consequently, the data can be easily contaminated by noise and thus unreliable for long term monitoring. In recent years, borehole resistivity has gained more favour for better depth of investigation, sense of target geometry and repeatability as conditions down a borehole are much more stable than that of on the surface (Daniels and Dyck, 1984, Shima, 1992, Zhou and Greenhalgh, 2000). As a result, in addition to mineral exploration, borehole resistivity methods, both single borehole profiling and cross borehole electrical resistivity tomography (ERT) have been used extensively in environmental and geotechnical monitoring (LaBrecque et. al., 1996, Muller, et. al., 2010, Nimmer, et. al., 2007, Ward, 1990).

Although the capability of resistivity methods in dealing with exploration and monitoring problems has been demonstrated, previous studies generally assume the boreholes are drilled near vertically and in the same plane for cross borehole ERT. However, for practical reasons, boreholes are usually not drilled vertically and different boreholes have different azimuths (for example inclined and horizontal drilling). Oldenborger et. al., 2005 have demonstrated that electrode mislocations could result in systematic errors well above typical data noise level. It is also shown in Yi et al., 2009 that borehole deviation effect may cause significant artifacts in inversion results. Therefore, assuming vertical boreholes rather than the actual inclined configurations could raise errors that are problematic in resolving high resolution structures and monitoring long term time-varying changes. We propose that, for near surface borehole resistivity surveys, accurate array locations and correct geometry factors should be obtained to account for borehole deviation effect and for accurate imaging or monitoring.

Method

For resistivity surveys in near-surface boreholes (both single borehole profiling and cross borehole ERT), we are dealing with a transition from half-space to full-space scenarios. On the surface of a homogeneous half-space, all injected currents are restricted to flow into the Earth. With depth, it transits into to full-space case where injected currents are free to flow in all directions (Figure 1). As a result, a geometry factor for full-space case is essentially twice the half-space case.

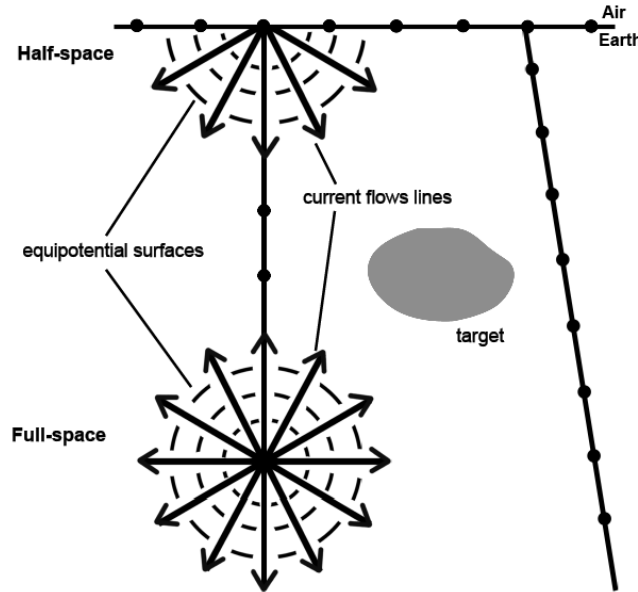


Figure 1. Schematic plot of surface and borehole electrode layout for either imaging or monitoring. Black solid circles represent surface and borehole electrodes.

In measuring bulk resistivity, a pair of current electrodes is used to inject current I into surrounding materials. The resulting potential difference ΔV at another pair of electrodes is measured (Figure 2(a)). Electrode array pairs are moved along the borehole(s) for profiling and ERT. The apparent resistivity ρ_a can be calculated from

$$\rho_a = \frac{\Delta V}{I} k \quad (1)$$

where k is geometry factor for a certain electrodes array configuration.

For an electrode array AB-MN along a near-surface borehole (Figure 2(a)), electrical images A' and B' are induced with equal current strength at equal distances to the air-Earth interface above the Earth (Van and Cook, 1966). Both electrical images will also results in potentials at M and N. Then the potential difference between M and N

$$\Delta V = \frac{\rho_a I}{4\pi} \left(\frac{1}{AM} + \frac{1}{A'M} - \frac{1}{BM} - \frac{1}{B'M} - \frac{1}{AN} - \frac{1}{A'N} + \frac{1}{BN} + \frac{1}{B'N} \right) \quad (2)$$

and apparent resistivity can be calculated from equation 1 with geometry factor

$$k = 4\pi / \left(\frac{1}{AM} + \frac{1}{A'M} - \frac{1}{BM} - \frac{1}{B'M} - \frac{1}{AN} - \frac{1}{A'N} + \frac{1}{BN} + \frac{1}{B'N} \right) \quad (3)$$

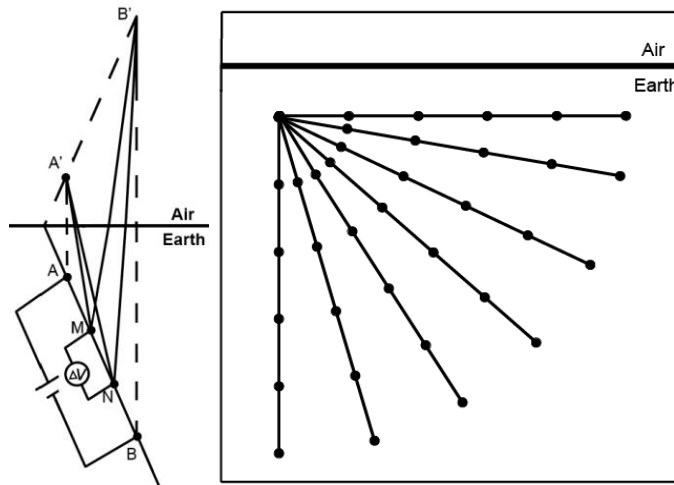


Figure 2(a), (left) Electrodes array AB-MN and induced images. Current is injected at A (positive) and sink at B (negative). A', B' are induced electrical images. Overall potential difference between M and N is measured. (b). (right) Schematic plot of near surface boreholes at different dip angles. Black solid circles represent borehole electrodes.

To examine the deviation effect in geometry factors, we define a normalized geometry factor by dividing geometry factor (k) along boreholes at various dip angles by full-space and vertical cases (k_v).

$$\hat{n}_k = k/k_v \quad (4)$$

For boreholes with different dip angles as depicted in Figure 2(b), geometry factors normalized by full-space and vertical cases for Schlumberger array are depicted in Figure 3 and Figure 4, respectively.

Figure 3 shows the transition of geometry factors from half-space ($\hat{n}_k = 0.5$) to full-space scenario ($\hat{n}_k = 1.0$). For shallow dipping boreholes, in particular, the normalized geometry factors show larger variations and change into full-space case at deeper depth along borehole.

Figure 4 shows that, in general, the normalized geometry factors converges to 1.0 as the electrode array moves deeper into the borehole and geometry factors along shallow dipping boreholes have greater variations than those along near vertical boreholes. As the dip angle decreases towards horizontal, \hat{n}_k converges to 1.0 at deeper depth. For the 16m electrode spacing case, at dip angle of 80 degrees, the maximum deviation from vertical is within 1%, which is below data noise level. For a near horizontal borehole dipping at 10 degrees, on the other hand, \hat{n}_k starts from 0.66 at 30 m and the deviation only gets below noise level after the first 280m. This is mainly because, for a near horizontal borehole, the induced electrical images along the profile stay to be close to the voltage electrodes and potentials from these images remain significant to overall potential differences. Therefore, borehole deviation effect is especially important for shallow dipping boreholes.

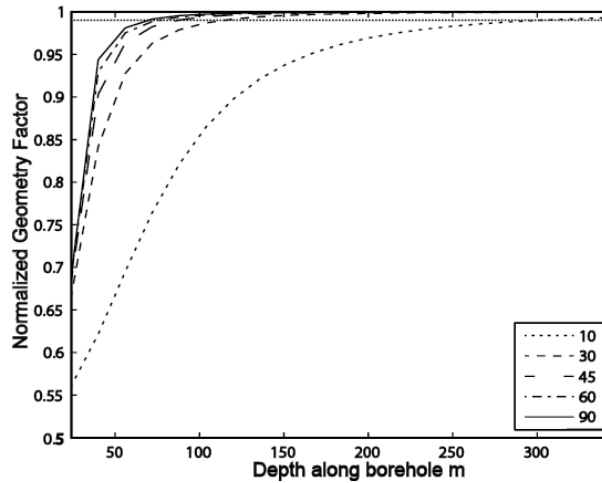


Figure 3. Geometry factors along boreholes dipping at various angles (in degrees) normalized by full-space cases. The horizontal dotted line is typical data noise level (1%). 0.5 corresponds to half-space case and 1.0 correspond to full-space case.

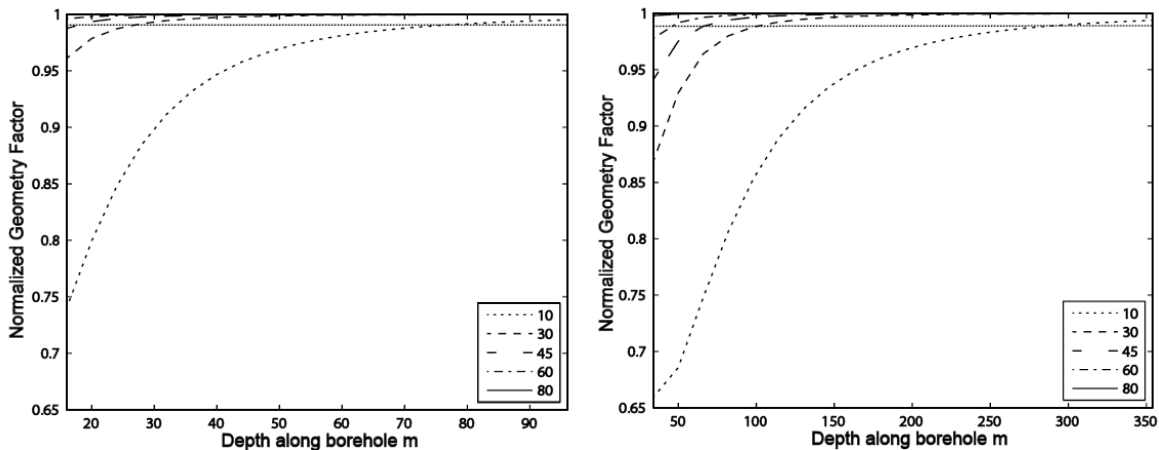


Figure 4. Geometry factors along boreholes dipping at various angles (in degrees) normalized by vertical cases. Electrodes are at 4m (left) and 16m (right) spacing. The horizontal dotted line is typical data noise level. $\hat{n}_k=1.0$ is when the actual geometry factors converges to that of vertical cases.

Examples

In order to evaluate the importance of geometry factors on actual data, a resistivity profiling survey is conducted under a lake at Deep River, northern Ontario. The borehole cable is laid out at the bottom of the lake which deviates from horizontal at approximately 10 degrees from the shore to the centre (Figure 5). There are 24 electrodes at 4m spacing lined up along a borehole cable.

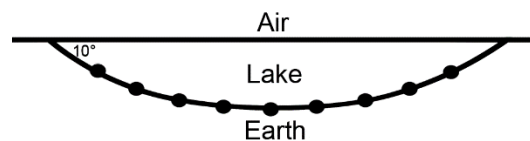


Figure 5. Schematic plot of electrode layout at bottom of the lake.

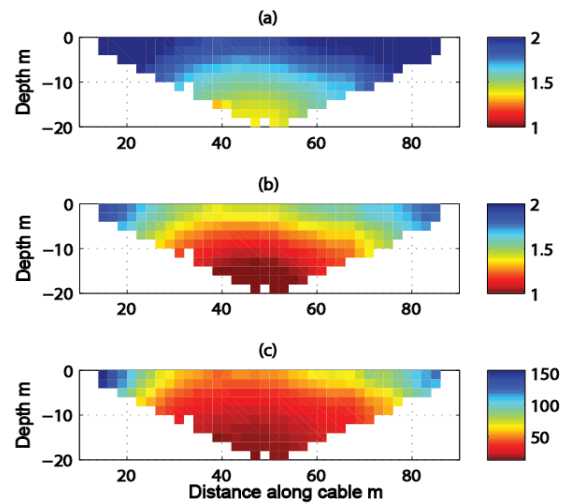


Figure 6. Apparent resistivity pseudo-sections in ohm-m (a) assuming the cable is laid out horizontally (with horizontal geometry factors k_h); (b) calculated with deviation effect and correct geometry factors k ; (c) difference between $\rho_a(k_h)$ and $\rho_a(k)$. (a), (b) are in logarithmic scale while (c) is in linear scale.

Comparing Figure 6 (a) and (b), it is observed that both $\rho_a(k_h)$ and $\rho_a(k)$ show a similar resistivity variation pattern of the materials getting more conductive with depth. However, $\rho_a(k)$ is generally smaller than $\rho_a(k_h)$ and shows larger variations. Their difference is about 66% of $\rho_a(k)$, which sits well above data noise level.

Conclusions

For near surface borehole resistivity surveys, geometry factors transit from half-space to that of full-space cases as the electrode arrays move from top to bottom of boreholes. Difference in apparent resistivity calculated with and without correct geometry factors, especially for near horizontal boreholes, sits well above typical data noise level. Therefore, in a near surface borehole resistivity survey, it is of great importance to obtain accurate electrode array locations and correct geometry factors in order to accurately image or monitor target structures,

Acknowledgements

This research is funded by SUMIT ORF project coordinated by Centre for Excellence in Mining Innovation (CEMI) and by National Science and Engineering Research Council of Canada (NSERC). The multi-electrode borehole cable and data acquisition system was developed by Geoserve in Germany.

References

- Muller, K., Vanderborghy, Jan., Englert, A., Kemna, A., Huisman, J.A., Ring, J., & Vereecken, H., 2010. Imaging and characterization of solute transport during two tracer tests in a shallow aquifer using electrical resistivity tomography and multilevel groundwater samplers, *Water Resour. Res.*, 46, W03502, doi:10.1029/2008WR007595.
- Daniels, J.J. and Dyck, A., 1984, Borehole resistivity and electromagnetic methods applied to mineral exploration. *IEEE Transactions on Geoscience and Remote Sensing*, GE-22, 80-87.
- Ramirez, A., Daily, W., LaBrecque, D., Owen, E. and Chesnut, D., 1993. Monitoring an underground steam injection process using electrical resistance tomography, *Water Resour. Res.*, 29, 73–87.
- LaBrecque, D.J., Ramirez, A.L., Daily, W.D., Binley, A.M., & Schima, S.A., 1996 ERT monitoring of environmental remediation processes *Meas. Sci. Technol.*, 7, 375 doi:10.1088/0957-0233/7/3/019.
- Nimmer, R. E., Osiensky, J. L., Binley, A. M., Sprenke, K. F., & Williams, B. C., 2007. Electrical resistivity imaging of conductive plume dilution in fractured rock. *Hydrogeology Journal*, 15(5), 877-890. doi:10.1007/s10040-007-0159-z.

- Oldenborger, G.A., Routh, P.S., & Knoll, M.D., 2005, Sensitivity of electrical resistivity tomography data to electrode position errors. *Geophysical Journal International*, 163, 1–9.
- Shima, H., 1992, 2D and 3D resistivity imaging reconstruction using cross-hole data, *Geophysics*, 55, 682-694.
- Yi, M.J., Kim, J.H. & Son, J.S., 2009. Borehole deviation effect in electrical resistivity tomography. *Geosciences Journal*, vol. 13, No. 1, p. 87 102, doi:10.1007/s12303-009-0008-2.
- Van, N. R., & Cook, K. L., 1966. Interpretation of resistivity data. Washington: U.S. Govt. Print. Off.
- Ward, S.H., 1990. Geotechnical and environmental geophysics. Tulsa, Okla: Society of Exploration Geophysics. Vol. 1.
- Zhou, B. and Greenhalgh S. A., 2000, Cross-hole resistivity tomography using different electrode configuration, *Geophysical Prospecting*, 48 (5), 887-912.